

## Atomic-scale composition fluctuations in III-V semiconductor alloys

H. W. M. Salemink and O. Albrektsen\*

*IBM Research Division, Zurich Research Laboratory, CH-8803 Rüschlikon, Switzerland*

(Received 24 February 1993)

Composition fluctuations in epitaxially grown III-V compound semiconductor alloys are observed with atomic resolution in direct space. A tunneling microscope technique is employed on the (110) cross-sectional plane of epitaxially grown InGaAsP-InP and AlGaAs-GaAs multilayers cleaved in ultrahigh vacuum. The tunneling polarity is used to image the filled-state group-V (As,P) sublattice in InGaAsP and the empty-state group-III (Al,Ga) sublattice in AlGaAs. In both compounds, the atomic-scale variations observed in the charge density reflect the composition fluctuations in the respective sublattices: an attempt is made to identify different elements of similar valence (Al,Ga). The definition of the heterojunction interface can be directly assessed on the atomic scale.

The atomic distribution of the different elements in semiconductor compounds like AlGaAs and InGaAsP is of interest from the standpoint of basic semiconductor physics and for its implications in future device technology. The distribution of the elements over the atomic sites in such compounds is largely responsible for the variations of the electronic properties such as band-gap energy, Fermi energy, and electron confinement levels.<sup>1-3</sup> The spatial changes in the electronic band structure at semiconductor interfaces are strongly related to the valence occupancy of atomic sites in an environment of nanometer dimensions.<sup>2-4</sup>

At semiconductor interfaces (for instance, that of GaAs-AlGaAs), such alloy fluctuations are fundamental to the interfacial "roughness" and explain why no well-defined interface can exist on the atomic scale.<sup>2</sup> Another important issue is the variation in the semiconductor band-gap energy with the degree of local order.<sup>5</sup> The conventional experimental techniques used to study semiconductor interfaces, such as high-resolution transmission electron microscopy<sup>6,7</sup> (HRTEM) and photoluminescence<sup>8</sup> inevitably derive their information from a large number of unit cells (typically  $10^2$  and  $10^6$  for these two techniques, respectively) and therefore yield averaged data. Such a resolution will not be sufficient for nanometer-size structures. There are few theoretical investigations of the composition fluctuations because of the unknown distribution of atomic species over the lattice sites in ternary and quaternary compounds. The theoretical treatment of a random alloy would require far larger unit cells than the relatively small and regular sets used in today's numerical calculations.<sup>9</sup> To avoid this problem, an averaged (virtual) crystal potential is employed to describe the ternary alloys in the band-structure calculations of binary-ternary interfaces.<sup>3</sup>

In this paper we present data on the group-III and group-V sublattice occupancy in epitaxially grown III-V compounds: the composition fluctuations and interface definition are observed with atomic resolution in direct space.

The GaAs/Al<sub>x</sub>Ga<sub>1-x</sub>As/GaAs ( $x=0.35-0.38$ ) multilayers discussed here are grown by molecular-beam epitaxy (MBE) at 620 °C without growth interruption. The

AlGaAs material is highly *p* doped with Be at  $5 \times 10^{18} \text{ cm}^{-3}$  and the *p* doping of GaAs is  $1 \times 10^{19} \text{ cm}^{-3}$ . The In<sub>0.25</sub>Ga<sub>0.75</sub>As<sub>0.5</sub>P<sub>0.5</sub>/InP layers are grown by vapor-phase epitaxy (VPE) at 630 °C and *n* doped with Si at  $1 \times 10^{18} \text{ cm}^{-3}$ . The (001) substrates are nominally oriented 2.0° off the  $\langle 001 \rangle$  growth direction. Segments of the wafers are carefully aligned and cut, degassed in an ultrahigh vacuum (UHV) preparation chamber and subsequently cleaved to expose the (110) cross-sectional plane of the multilayer stack under an ambient pressure of  $1 \times 10^{-10}$  mbar. After transfer of the sample into the interconnected UHV scanning tunneling microscope (STM), which operates at a base pressure of  $< 4 \times 10^{-11}$  mbar, the STM tip is positioned right on the cross section of the multilayer stack (typical total thickness of 0.5 μm), using a VG HB100 scanning electron microscope (SEM).<sup>10</sup> This unique combination of UHV-STM/SEM is extremely useful for assessing the quality of cleaves through such epitaxial structures as well as for surveying the tip apex shape. Furthermore, it allows a rapid and direct positioning of the tunneling tip at a specific position with an accuracy of  $< 0.1 \mu\text{m}$ .

Owing to the properties of the (110) nonpolar cleavage plane in GaAs, which contains both Ga and As atoms in a  $1 \times 1$  unit cell arrangement, the tunnel polarity can be used selectively to image either the empty, group-III related Ga states or the filled, group-V related As states<sup>11,12</sup> (Fig. 1). The same argument holds for the equivalent (110) faces of other III-V compounds such as InP. No surface states in the fundamental band gap are observed on the clean (110) surface of the binary III-V compounds. Regarding ternary and quaternary material, no STM studies are reported, owing to the difficulty of accessing the small cross sections of the submicrometer-sized epitaxial samples: as such this technique provides a way to study these synthetic compounds. In earlier work, we have used this particular property of the III-V (110) surface to analyze the GaAs-AlGaAs interface in atomic detail by imaging the filled states of the As sublattice across the heterojunction.<sup>13</sup>

In this paper we present STM results for two types of multilayers: on the charge density of the *filled-state group-V* (As,P) sublattice across the InP-InGaAsP hetero-

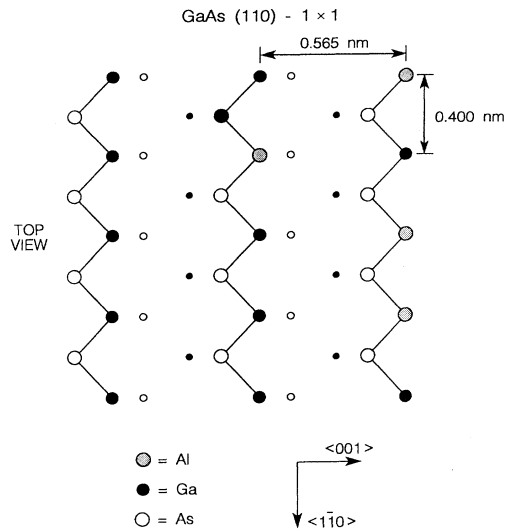


FIG. 1. Schematic arrangement of the group-III (Al,Ga) and the group-V (As) sites on the UHV cleaved (110) plane of a GaAs-AlGaAs interface. In the AlGaAs alloy, a fraction of the group-III Ga sites is replaced by Al atoms. Left column represents GaAs, middle and right column represent  $\text{Al}_{0.40}\text{Ga}_{0.60}\text{As}$ .

junction and on the distribution of the *empty-state group-III (Ga,Al)* states across the GaAs-AlGaAs heterojunction. The main observations are the following: the charge density corrugations of ternary and quaternary compounds vary on an atomic scale and, their variations are in marked contrast to the uniform charge density corrugation of binary materials. These fluctuations reflect the *distinct* atomic potentials of the alloy sublattices, namely, the group-V (As,P) sites in InGaAsP and the group-III (Al,Ga) sites in AlGaAs. Further findings are (1) in the AlGaAs material discussed here, the Al sites are not randomly distributed but show a tendency to form small, Al-rich clusters and (2) the lack of definition of the two interfaces of the AlGaAs layer on the atomic scale is observed directly, as reflected by the Al and Ga atomic distribution.

Figure 2 displays the group-V (As,P) sublattice on the cross-sectional (110) plane across the VPE-grown InP-In<sub>0.25</sub>Ga<sub>0.75</sub>As<sub>0.5</sub>P<sub>0.5</sub> multilayer interface, acquired at a sample voltage of  $-2.3$  V, representing the filled states. The different appearance of the two sides of the interface originates from uniform corrugation of the P atoms in InP, in contrast to the varying corrugations of the As and P atoms in InGaAsP. An abrupt transition is observed at the interface over plus or minus one unit cell in the  $\langle 001 \rangle$  growth direction. In the InGaAsP material the group-V sites nominally have an  $\text{As}_{0.5}\text{P}_{0.5}$  composition and their distribution over the lattice sites appears to be random on the (110) plane.

In the topography shown in Fig. 2, a step ledge one unit cell in height runs along the interface, separating two (110) terraces, one on InP and one on InGaAsP. This step is probably due to stress relief in the cleaving

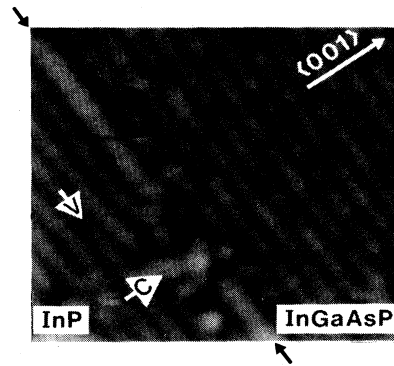


FIG. 2. Cross-sectional topograph of a VPE-grown InP-InGaAsP heterojunction. Sample voltage is  $-2.3$  V; the topograph displays the filled-state sublattice of (P) and (As,P) atoms in the InP and InGaAsP layers, respectively. The  $\langle 001 \rangle$  growth direction is indicated and the interface is marked with arrows. Note the alloy potential fluctuations in the (As,P) sublattice. A likely semiconductor cluster is marked by (C) and a single missing P atom by (V). Note the deflection of the empty-state orbitals into the vacancy site. The charge density of the P atoms at the step ledge is enhanced after accounting for the effect of the background subtraction.

process. The step ledge is responsible for the enhanced appearance of the P atoms at the interface, which are now less coordinated in their lattice and can exhibit some “charge spill-over.” Remarkably, the interface remains well defined in the presence of such a step. The defect (C) is probably a cluster of semiconductor material on the surface, and might originate from the terrace ledge: no surface contaminants like those found on the AlGaAs-GaAs stacks were detected,<sup>10</sup> due to the low oxygen sticking on these non-Al compounds. An interesting feature is the missing P atom in the InP, indicating a single P surface vacancy site: the filled-state orbitals of the neighboring P sites have “collapsed” noticeably into this empty lattice position, as seen by the inward bending of the  $\langle 1\bar{1}0 \rangle$  planes of up to 0.12 nm around the vacancy. This defect apparently affects electronically the arrangement of approximately 25 unit cells on the (110) plane.<sup>14</sup> On the GaAs (110) plane we do not observe such extended areas affected by a single missing site.

Figure 3 shows the charge density distribution of empty states on a (110) cross section of a multilayer stack containing nominal layers of 9.60-nm GaAs, 9.60-nm  $\text{Al}_{0.38}\text{Ga}_{0.62}\text{As}$ , and 4.8-nm GaAs. The sample voltage is  $+2.2$  V and the image represents the sublattice of the (group-III) Al and Ga sites. We note the uniform charge density corrugation of Ga atoms in both GaAs layers. By contrast, in the 17-unit-cells-wide AlGaAs layer we find—in addition to the chemisorbed defects<sup>10</sup>—an inhomogeneous charge density on the (Al,Ga) sublattice which distinctly displays two types of corrugation amplitude. Counting the number of small corrugations over 150 nm<sup>2</sup> of (110) AlGaAs material yields an Al fraction of 0.32, close to the nominal composition value of 0.38: these sites are attributed to the Al atomic charge

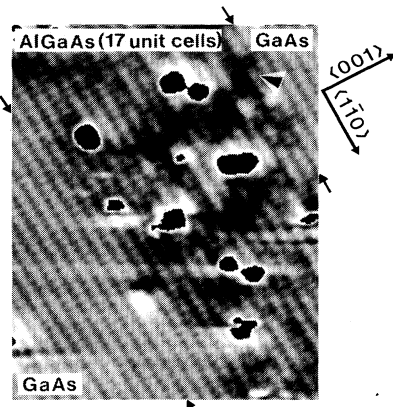


FIG. 3. Cross-sectional view of  $\langle 110 \rangle$  cleavage plane through GaAs-AlGaAs-GaAs multilayers. The  $\langle 001 \rangle$  growth direction is indicated and the approximate interfaces of the AlGaAs layer (17 unit cells wide, 9.605 nm) are indicated by arrows. Sample voltage is +2.2 V and the group-III sublattice is imaged (Ga atoms in GaAs, Al and Ga atoms in AlGaAs). The two distinct charge density patterns in the AlGaAs are attributed to Ga and Al atomic sites. Also note Al clustering in AlGaAs and the “roughness” of the AlGaAs-GaAs interface. The black spots are due to selective oxygen chemisorption on AlGaAs, which are clipped off in the contrast enhancing process (Ref. 13). The image is of unprocessed STM data. The higher atomic charge density amplitudes are assigned to Ga sites and the lower amplitudes to Al sites.

density. The fact that we observe distinct charge density amplitudes of the group-III (Al,Ga) sublattice in the Al-GaAs layer confirms the observation of the atomic-scale potential fluctuations. In Fig. 4 we have schematically drawn the energy diagram which applies to imaging the empty states of Fig. 3 where the AlGa states are displayed at a sample voltage of +2.2 V. Tunneling electrons are injected into the lower conduction-band (CB) states. Owing to their elemental character which is partly maintained on the  $1 \times 1$  surface, these lower CB states are uniquely connected to their elemental group-III origin (Al or Ga). In a similar way, the upper valence-band states are connected to the group-V As states. The Al states are energetically positioned (approximately 0.5 eV) higher than the Ga states as the Al states are more hy-

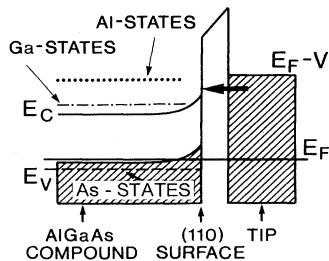


FIG. 4. Schematic energy diagram for tunneling into empty group-III states above the conduction-band edge of AlGaAs at positive sample voltage. The distinct contributions from localized Ga and Al conduction-band states are qualitatively indicated.

drogenlike (“lighter”); this is also reflected in the larger band gap of AlAs than that of GaAs. Hence, when tunneling occurs into the lower CB states at a given injection energy we expect a smaller current contribution for the Al sites and therefore a lower corrugation than for the Ga sites. This basic argument leads to the same identification as the previous site-counting argument and also associates the smaller corrugations with the Al sites. In reviewing the As-P sublattice in Fig. 2 we attribute the larger corrugation amplitudes to the As sites on similar arguments. We point out that our previous work<sup>13</sup> using the imaging of the As sublattice does not differentiate between the two elements directly but reflects the different electronic environment of the As sublattice. The work presented here thus shows the chemical differentiation within a valence group.

With this assignment of the different Al and Ga elements in the group-III sublattice we turn to the detail of the (inverted) AlGaAs-GaAs interface from Fig. 3 and show this zoomed area in detail in Fig. 5. The Al sites (low corrugation) are clearly seen at this particular interface. Two interesting features are (a) the clustering of five Al sites in the  $\langle 1\bar{1}0 \rangle$  direction (topmost AlGaAs lay-

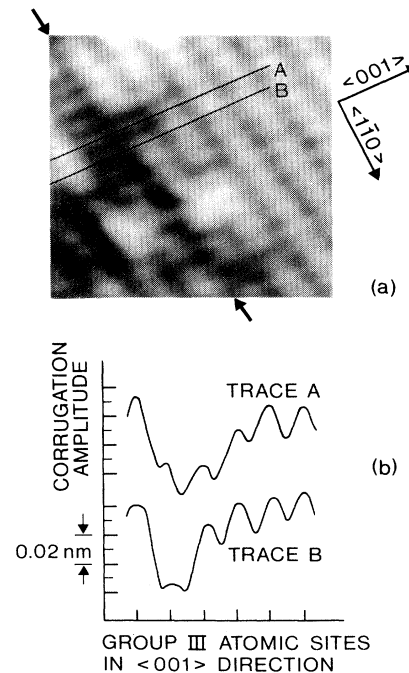


FIG. 5. (a) Detailed area of the (inverted) AlGaAs-GaAs interface from Fig. 3: the area is zoomed in the upper right part of Fig. 3. Note the difficulty in determining the interface at atomic resolution. The topograph represents the empty states of the Ga and Al atoms, at a sample voltage of +2.2 V. The darker areas with lower atomic corrugation relate to Al sites, as discussed in Fig. 4 and in the text. (b) Two empty-state corrugation profiles along lines A and B in (a), in the  $\langle 001 \rangle$  direction. The smaller amplitudes (two in line A, one in line B) are attributed to the Al sites. In the topmost AlGaAs layer, five Al sites cluster in the  $\langle 1\bar{1}0 \rangle$  direction; a single Al site is in the first GaAs layer.

er) and the single Al site embedded in the first GaAs layer. The respective corrugation profiles along lines *A* and *B* are given in Fig. 5(b). From Figs. 3 and 5 it is clearly seen that such high-resolution “chemical” mapping studies at semiconductor interfaces can significantly contribute to the outstanding issues of the “roughness” of interfaces, quantum wells, and confinement potentials. Atomic detail is possible as these data directly reveal the atomic sites. In similar alloys, subordering was previously detected by HRTEM electron diffraction<sup>5,15,16</sup> as additional diffraction spots. In one paper<sup>17</sup> specific atom imaging was reported with a combined setup of STM and optical excitation, but the contrast mechanism is not well understood.

The atomic structure (compound distribution) and electronic band structure (e.g., valence-band energy) are closely interrelated in crystalline solids; hence we believe that the alloy fluctuations as shown in Fig. 3 also account for the variations in the tunneling current-voltage (*I-V*) characteristics observed on the ternary AlGaAs,<sup>13,18</sup> where we find  $\pm 50$  meV fluctuations over a length scale of about 3 nm. With a band-gap dependence of 12.5 meV/(% Al fraction), we calculate an actual number of three to four Al sites within our tunneling filament, which covers approximately 10 unit cells in diameter ( $x_{\text{Al}}=0.35\pm 0.05$ ). In this context we note the deviations

from the mean composition of up to 5% over a spatial scale of  $\sim 15$  nm, as have been observed by an atom probe technique.<sup>19</sup>

In summary, we have observed the composition fluctuations of group-V (As,P) sites in InGaAsP and of group-III (Al,Ga) sites in AlGaAs with atomic resolution in direct space. An inhomogeneous group-III distribution is seen in the charge density of the AlGaAs layer and Al clustering is observed over a few unit cells. Such a phase separation of the AlGaAs in nanometer-sized GaAs and AlAs subunits was proposed on theoretical grounds.<sup>20</sup> The individual assignment of Al sites displays the possibility for chemical analysis in compound lattices and allows us to define an interface on the unit-cell scale: this delivers direct evidence of the ill-defined interface in such alloy compounds on the atomic scale and opens new ways to study the roughness of semiconductor interfaces in detail.

We acknowledge extensive discussions with S. Ciraci, E. Tosatti, and A. Baldereschi. For epitaxial growth of the multilayers we acknowledge the cooperation of H. Meier (MBE), D. J. Arent (MBE), and P. Roentgen (VPE). For expert material processing we are indebted to H. Richard and L. Perriard. J. Schmid cooperated with us in the early STM work on InP.

\*Also at Institute for Quantum Electronics, ETH Hönggerberg, CH-8093 Zürich, Switzerland; present address: Telecommunications Research Laboratory, DK-2970 Hørsholm, Denmark.

<sup>1</sup>J. E. Bernard, R. G. Dandrea, L. G. Ferreira, S. Froyen, S.-H. Wei, and A. Zunger, *Appl. Phys. Lett.* **56**, 731 (1990).

<sup>2</sup>S. B. Ogale, A. Madhukar, F. Voillot, M. Thomsen, W. C. Tang, T. C. Lee, J. Y. Kim, and P. Chen, *Phys. Rev. B* **36**, 1662 (1987).

<sup>3</sup>C. G. van de Walle and R. M. Martin, *Phys. Rev. B* **35**, 8154 (1987); A. Baldereschi, S. Baroni, and R. Resta, *Phys. Rev. Lett.* **61**, 734 (1988).

<sup>4</sup>*Heterojunction Band Discontinuities*, edited by F. Capasso and G. Margaritondo (North-Holland, Amsterdam, 1987).

<sup>5</sup>T. Suzuki, A. Gomyo, S. Iijima, K. Kobayashi, S. Kawata, I. Hino, and T. Yuasa, *Jpn. J. Appl. Phys.* **27**, 2098 (1988).

<sup>6</sup>J. Coleman, G. Costrini, S. Jeng, and C. Wayman, *J. Appl. Phys.* **59**, 428 (1986).

<sup>7</sup>A. Ourmazd, W. T. Tsang, J. A. Rentschler, and D. W. Taylor, *Appl. Phys. Lett.* **50**, 1417 (1987); A. Ourmazd, D. W. Taylor, J. Cunningham, and C. W. Tu, *Phys. Rev. Lett.* **62**, 933 (1989).

<sup>8</sup>J. Singh, K. Bajaj, and S. Chaudhuri, *Appl. Phys. Lett.* **44**, 805 (1984); M. Tanaka and H. Sakaki, *J. Cryst. Growth* **81**, 153 (1987).

<sup>9</sup>I. P. Batra, S. Ciraci, and A. Baratoff, in *Proceedings of the NATO Workshop on Condensed Systems and Low Dimensionality, Marmaris, Turkey, 1990*, Vol. 253 of *NATO Advanced Study Institute, Series B: Physics*, edited by J. L. Beeby (Plenum, New York, 1991), p. 557.

<sup>10</sup>O. Albrektsen and H. Salemink, *J. Vac. Sci. Technol. B* **9**, 779 (1991).

<sup>11</sup>D. J. Chadi, *Phys. Rev. B* **19**, 2074 (1979).

<sup>12</sup>R. M. Feenstra, J. A. Stroscio, J. Tersoff, and A. P. Fein, *Phys. Rev. Lett.* **58**, 1192 (1987).

<sup>13</sup>O. Albrektsen, D. J. Arent, H. P. Meier, and H. W. M. Salemink, *Appl. Phys. Lett.* **57**, 31 (1990).

<sup>14</sup>L. J. Whitman, J. A. Stroscio, R. A. Dragonset, and R. J. Celotta, *J. Vac. Sci. Technol. B* **9**, 770 (1991).

<sup>15</sup>P. M. Petroff, A. Y. Cho, F. K. Reinhart, A. C. Gossard, and W. Wiegmann, *Phys. Rev. Lett.* **48**, 170 (1982).

<sup>16</sup>T. S. Kuan, W. I. Wang, and E. L. Wilkie, *Appl. Phys. Lett.* **51**, 51 (1987); T. S. Kuan, T. F. Kuech, W. I. Wang, and E. L. Wilkie, *Phys. Rev. Lett.* **54**, 210 (1985).

<sup>17</sup>L. L. Kazmerski, *J. Vac. Sci. Technol. B* **9**, 1549 (1991).

<sup>18</sup>H. W. M. Salemink, O. Albrektsen, and P. Koenraad, *Phys. Rev. B* **46**, 6946 (1992) and (unpublished).

<sup>19</sup>R. A. D. Mackenzie, J. A. Liddle, and C. R. M. Grovenor, *J. Appl. Phys.* **69**, 250 (1991).

<sup>20</sup>S. Ciraci and I. Batra, *Phys. Rev. B* **36**, 1225 (1987).

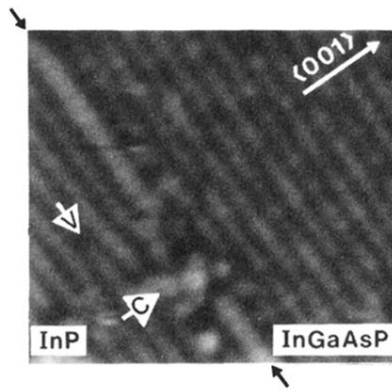


FIG. 2. Cross-sectional topograph of a VPE-grown InP-InGaAsP heterojunction. Sample voltage is  $-2.3$  V; the topograph displays the filled-state sublattice of (P) and (As,P) atoms in the InP and InGaAsP layers, respectively. The  $\langle 001 \rangle$  growth direction is indicated and the interface is marked with arrows. Note the alloy potential fluctuations in the (As,P) sublattice. A likely semiconductor cluster is marked by (C) and a single missing P atom by (V). Note the deflection of the empty-state orbitals into the vacancy site. The charge density of the P atoms at the step ledge is enhanced after accounting for the effect of the background subtraction.

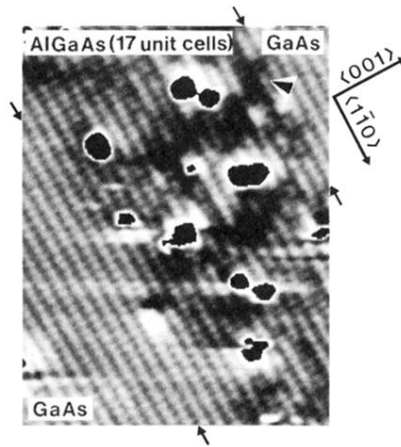


FIG. 3. Cross-sectional view of  $\langle 110 \rangle$  cleavage plane through GaAs-AlGaAs-GaAs multilayers. The  $\langle 001 \rangle$  growth direction is indicated and the approximate interfaces of the AlGaAs layer (17 unit cells wide, 9.605 nm) are indicated by arrows. Sample voltage is +2.2 V and the group-III sublattice is imaged (Ga atoms in GaAs, Al and Ga atoms in AlGaAs). The two distinct charge density patterns in the AlGaAs are attributed to Ga and Al atomic sites. Also note Al clustering in AlGaAs and the “roughness” of the AlGaAs-GaAs interface. The black spots are due to selective oxygen chemisorption on AlGaAs, which are clipped off in the contrast enhancing process (Ref. 13). The image is of unprocessed STM data. The higher atomic charge density amplitudes are assigned to Ga sites and the lower amplitudes to Al sites.

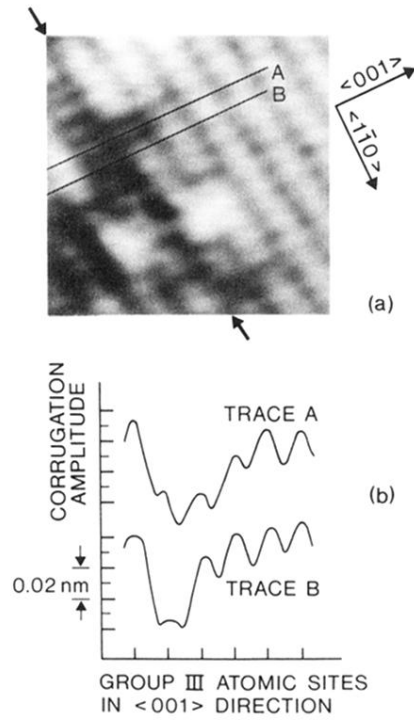


FIG. 5. (a) Detailed area of the (inverted) AlGaAs-GaAs interface from Fig. 3: the area is zoomed in the upper right part of Fig. 3. Note the difficulty in determining the interface at atomic resolution. The topograph represents the empty states of the Ga and Al atoms, at a sample voltage of +2.2 V. The darker areas with lower atomic corrugation relate to Al sites, as discussed in Fig. 4 and in the text. (b) Two empty-state corrugation profiles along lines *A* and *B* in (a), in the  $\langle 001 \rangle$  direction. The smaller amplitudes (two in line *A*, one in line *B*) are attributed to the Al sites. In the topmost AlGaAs layer, five Al sites cluster in the  $\langle 1\bar{1}0 \rangle$  direction; a single Al site is in the first GaAs layer.